DESIGN SYNTHESIS OF ADAPTIVE MESOSCOPIC CELLULAR STRUCTURES WITH UNIT TRUSS APPROACH AND PARTICLE SWARM OPTIMIZATION ALGORITHM

Hongqing Vincent Wang [a]	Chris Williams [b]	David W. Rosen [b]*
R&D Engineer	Research Assistant	Professor

[a] IronCAD Inc., 700 Galleria Parkway, Suite 300, Atlanta, GA 30339
[b] The George W. Woodruff School of Mechanical Engineering, Georgia Institute of Technology Atlanta, GA 30332

* Corresponding Author: 404-894-9668, david.rosen@me.gatech.edu.

ABSTRACT

Cellular material structures have been engineered at the mesoscopic scale for high performance and multifunctional capabilities. However, the design of adaptive cellular structures - structures with cellular configurations, sizes, and shapes designed for a specific geometric and loading context - has not been sufficiently investigated. In this paper, the authors present a design synthesis method with the use of unit truss approach and particle swarm optimization algorithm to design adaptive cellular structures. A critical review is presented to show the pros and cons of the new design synthesis method and an existing homogenization method. The research extends the application of additive manufacturing in the design of new materials for high performances and benefits its long-term growth.

KEY WORDS

Mesoscopic Cellular Structure, Adaptive Cellular Structure, Design Synthesis, Unit Truss, Particle Swarm Optimization, Homogenization Method, Additive Manufacturing

1 CELLULAR MATERIALS WITH DESIGNED MESOSTRUCTURE

More than 50 years of research have been dedicated to the development of design and manufacturing methods that are capable of applying the advantages of cellular materials found in the natural world to engineered artifacts. Much like wood, bone, and coral, man-made materials with cellular mesostructure (cells on the order of 0.1 to 10mm) such as foams, honeycombs, and lattices feature gaseous voids that are thoroughly dispersed throughout the solid phase of its body [1]. The key advantage offered by cellular materials is their high strength and relatively low mass. The concept of artificial cellular materials with designed mesostructure is motivated by the desire to put material only where it is needed for a specific application. An increase in strength and decrease in relative density are laudable benefits of this motivation; however, mesostructured materials are promising because they can be designed and manufactured for specific, multiple design objectives and product functions.

Due to the limitations found in traditional manufacturing technology, most available engineered lightweight structural cellular materials are linear patterns of primitives. With the advance of additive manufacturing technologies, however, engineers have the freedom to design structural cellular materials to provide stiffness, energy absorption characteristics, and good thermal and acoustic

insulation properties by orienting strut directions and adjusting strut diameter and cross-section (Figure 1a) [2]. Seepersad and coauthors, for example, designed the topology of an extruded cellular material to find the best compromise between heat transfer and part strength in a structural heat exchanger application [3]. Williams and coauthors investigated additive manufacturing processes and selected Selective Laser Melting and Three-Dimensional Printing for the manufacture of parts with metallic designed mesostructure [4].

Compliant mechanisms, another type of cellular structure (Figure 1b), can be designed to transform motions, forces, or energy by elastic deformation as opposed to traditional mechanisms consisting of rigid links [5-7]. Living organisms such as cartilage and living cells are sophisticated compliant mechanisms and they possess both a high degree of moving freedom and the ability to manipulate that freedom [8, 9]. Compliant mechanisms in nature are able to carry out diverse and soft movements. Most engineered compliant mechanisms are limited due to inferior design methods for complicated mechanisms that do not simultaneously consider axial forces, bending, torsion, nonlinearity, or buckling. Most compliant mechanisms can only carry out relatively simple movement compared to living organisms.

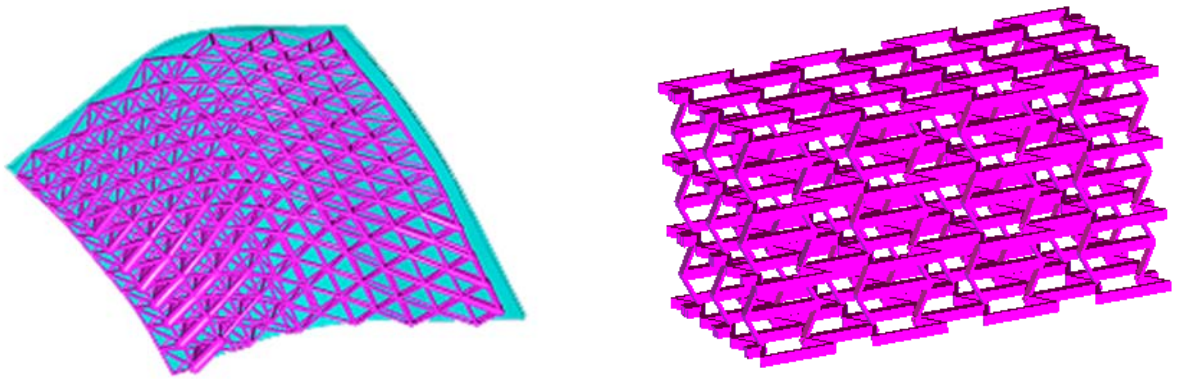

a. A lightweight truss structure supporting car body for high strength and minimum deflection

b. A compliant mechanism as a new material structure with negative Poisson's ratio

Figure 1. Examples of cellular structures

Cellular structures are called "adaptive" if their configuration, geometry, and sizes are chosen to significantly enhance the structures' performance, while conforming to the shape of parts they are embedded within or of neighboring parts. The systematic design of adaptive cellular structures has not been studied extensively. In this paper the authors propose a method for the design synthesis of adaptive cellular structures. Specifically, a synthesis method using a unit truss approach and integrated with particle swarm optimization is developed to systematically design adaptive mesoscopic cellular structures. The core components of the design method, the unit truss approach and particle swarm optimization method, are presented in Sections 2 and 3, respectively. The integration of these core constructs is described in Section 4. In Section 5, the method is validated through its application to a cantilever beam example and its comparison against the homogenization method with optimality criteria. Finally, in Section 6, the methodology is tested against a more complex example inspired by a morphing wing technology. The closure is offered in Section 7.

2 UNIT TRUSS APPROACH

A few structural analysis approaches have been developed to analyze compliant mechanisms. Typical methods include the ground truss (discrete) approach and the homogenization (continuum)

method. The ground truss approach can only provide a rough estimate for the geometry of designed structures [10-12]. The homogenization method achieves better results by using artificial unit cells; however, it may result in non-realizable elements and can be computationally expensive [13, 14].

We propose the unit truss, a new type of unit cell, to analyze cellular structures. The unit truss consists of the central node and a set of the half-struts that are connected to that node. An example of a unit truss is shown in Figure 2 [15]. This new unit cell approach was developed to accurately and efficiently analyze lightweight structures and compliant mechanisms, and to support their systematic design. The unit truss is leveraged from the ground truss approach and homogenization method. A microstructure cell is used to represent the material distribution in the homogenization method. An advantage of the unit truss is that it can be used as both the cell primitive for analysis and synthesis. Furthermore, the unit cell is manufacturable, whereas the microstructures in the homogenization method are artificial and not manufacturable [16].

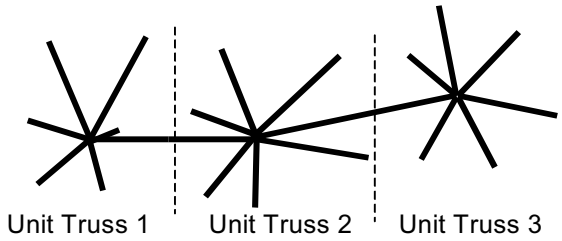

Figure 2. Definition of unit truss

In order to analyze conformal cellular structures, the mechanics model of unit trusses was successfully developed. As shown in the stress plot of a sample unit truss in Figure 3, the strain and stress around the nodes are complicated due to considerable inter-strut interactions and large bending moments [15]. As such, the unit truss model includes considerations of axial forces, bending, torsion, nonlinearity, and buckling [15].

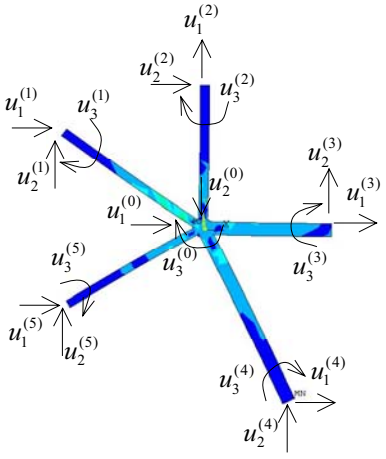

Figure 3. Using unit truss

The constitutive equations of 2-D and 3-D unit trusses are derived using beam theory as shown in Equations 1-3. $\underset{\sim}{K}_e$ denotes the linear elasticity of a unit truss, while $\underset{\sim}{U}$ and $\underset{\sim}{F}$ represents the nodal displacements and forces. Each strut is modeled as a conventional frame element from finite element analysis methods; however, we have added provisions for modeling geometric and material

nonlinearities, as well as geometric interactions at nodes. Unit trusses can have any number of incident struts. They can be thought of as special elements with which to analyze large cellular structures using methods similar to conventional finite element methods. The geometric interactions between struts at nodes are adjusted by correcting the diagonal component in the stiffness matrix $\underset{\sim}{K}_e$.

Static equilibrium: $\underset{\sim}{K}_e \cdot \underset{\sim}{U} = \underset{\sim}{F}$ Equation 1

Stiffness: $$[\underset{\sim}{K}_e] = \begin{bmatrix} \sum_{i=1}^{N} \Phi_{11}^{(i)} & \Phi_{12}^{(1)} & \Phi_{12}^{(2)} & \cdots & \Phi_{12}^{(N)} \\ \Phi_{21}^{(1)} & \Phi_{22}^{(1)} & 0 & \cdots & 0 \\ \Phi_{21}^{(2)} & 0 & \Phi_{22}^{(2)} & \cdots & 0 \\ \vdots & \vdots & \vdots & \ddots & \vdots \\ \Phi_{21}^{(N)} & 0 & 0 & \cdots & \Phi_{22}^{(N)} \end{bmatrix}_{3(N+1)\times 3(N+1)}$$ Equation 2

Nodal displacements: $$[\underset{\sim}{U}] = \left[\begin{bmatrix} u^{(0)} \\ \sim \end{bmatrix} \quad \begin{bmatrix} u^{(1)} \\ \sim \end{bmatrix} \quad \cdots \quad \begin{bmatrix} u^{(N)} \\ \sim \end{bmatrix} \right]^T$$

Nodal forces: $$[\underset{\sim}{F}] = \left[\begin{bmatrix} f^{(0)} \\ \sim \end{bmatrix} \quad \begin{bmatrix} f^{(1)} \\ \sim \end{bmatrix} \quad \cdots \quad \begin{bmatrix} f^{(N)} \\ \sim \end{bmatrix} \right]^T$$ Equation 3

Geometric nonlinearity occurs in structures undergoing large displacements or rotations, large strains, or a combination of these. Material nonlinearity occurs due to nonlinear stress-strain behavior. Geometric and material nonlinearities are considered with the tangent stiffness method. The tangent stiffness method is a linearization approach to analyze the nonlinear behavior of compliant mechanisms. Linear elasticity theory is used to solve nonlinear problems. The behavior of an elastic unit truss can be traced back incrementally using Equation Equation 4, which is in a linear form [17]. $\underset{\sim}{K}_t$ is the tangent stiffness matrix, $d\underset{\sim}{U}$ are the incremental nodal displacements, and $d\underset{\sim}{F}$ are the incremental nodal forces. Both geometric and material elastic nonlinearities are considered using Equation Equation 5. The linear elastic stiffness is designated as $\underset{\sim}{K}_e$, while $\underset{\sim}{K}_g$ and $\underset{\sim}{K}_m$ represent geometric nonlinear stiffness and material nonlinear stiffness, respectively [17].

$$\underset{\sim}{K}_t \bullet d\underset{\sim}{U} = d\underset{\sim}{F}$$ Equation 4

$$\underset{\sim}{K}_t = \underset{\sim}{K}_e + \underset{\sim}{K}_g + \underset{\sim}{K}_m$$ Equation 5

Compared to the ground truss approach, which is typical of topology optimization methods [2], our unit truss approach provides better accuracy to analyze compliant mechanisms by simultaneously analyzing multiple-degree-of-freedom deformation and considering nonlinearity. Compared to the homogenization method, the unit truss approach is more efficient due to fewer microstructures used for analysis. As a result of this research, the analysis of lightweight structures and compliant mechanisms can utilize the same mechanics model (unit truss). This enables us to design structures for both stiffness and compliance simultaneously.

3 PARTICLE SWARM OPTIMIZATION

The design synthesis of adaptive cellular structures is a large-scale nonlinear problem with multiple objectives and a mixed-discrete design space. The design problem formulations for lightweight structures and compliant mechanisms are shown in Figure 4. Strut sizes (diameter for cylindrical struts or width for 2-D rectangular struts) are the design variables represented by

$x_i (i = 0,1,...,n)$, where n is the number of struts in the starting structure topology. The constraints include the bounds on strut diameters, static equilibrium, and stress. The objectives are to minimize the normalized Mean Squared Deviation $(\text{mean}(SD_k))_{norm}$ between the desired shape and the actual shape under deformation, and to minimize the normalized total material volume V_{norm} [18]. Detailed explanation of this design problem is given in the next section.

Particle Swarm Optimization (PSO) and Genetic Algorithms (GA) were selected from available optimization algorithms to systematically search for design solutions. PSO shares similarities with GA, while PSO enables cooperative behavior among individual design instances as well as the competition modeled using GA. Hence, PSO often converges more quickly than GA and was selected for the design synthesis of cellular structures [19].

Find: Diameters of lattice struts

$$x = \{x_1, x_2, \cdots, x_n\}$$

Satisfy:

Bounds: $x_i \in \{0, [x_{\min}, x_{\max}]\}$

Constraints:

static equilibrium $h_1 : K \bullet U = F$

$$U|_{x_i=0} = 0$$

$$F|_{x_i=0} = 0$$

axial stress $g_1 : \sigma_{axial,i}(\mathrm{x}) \le \sigma_{\mathrm{y}}$

total material volume

$$g_2 : V_{total} \le V_{total,\max}$$

Minimize:

maximum nodal deflection $\max(U)$

a. Lightweight structures

Find: Strut widths

$$x = \{x_1, x_2, \cdots, x_n\}$$

Satisfy:

Bounds: $x_i \in \{0, [x_{\min}, x_{\max}]\}$

Constraints:

static equilibrium - $h_1 : K_t \bullet dU = dF$

$$U|_{x_i=0} = 0$$

$$F|_{x_i=0} = 0$$

stress - $g_1 : \sigma(\mathrm{x}) \le \sigma_{\max}$

Minimize:

mean squared deviation and material volume

$$f(x,U) = w_1 \times (\text{mean}(SD_k))_{norm} + w_2 \times V_{norm}$$

b. Compliant mechanism

Figure 4. Problem formulation for cellular structures

Conceptually, PSO simulates the movement of birds in a flock, where individuals adjust their flying according to their experience and other individuals' experiences during searches for food [20]. It starts with global search and then gradually shifts to local search through the change of weight coefficient. Each of the p particles (birds), which represent design instances, is given an initial position and velocity. In the context of this design problem, an initial position corresponds to a set of strut diameter values for the entire mechanism and the velocity is the change rate of the strut diameters between design iterations. The key step in the PSO algorithm is the update of the velocity from one iteration to the next. The new velocity is given as a combination of the current velocity, a velocity change based on the particle's learning, and a velocity change based on the flock's behavior (social learning) as given in Equation 6.

$$v_i = \underbrace{w_k \times v_i}_{\text{velocity inertia}} + \underbrace{\varphi_1 \times rand() \times (p_i - x_i)}_{\text{cognition behavior}} + \underbrace{\varphi_2 \times rand() \times (p_g - x_i)}_{\text{social behavior}} \qquad \text{Equation 6}$$

where, w_k = velocity inertia weight, φ_1 is the cognition learning factor, φ_2 is the social learning factor, *rand*() generates a random value in the range [0, 1], p_i is the best position of particle i, and p_g is the best position of any particle. Positions are computed simply using Equation 7. During each iteration, all particles' velocities and positions are updated, and then the objective function is computed. Convergence is checked by considering changes in objective function values, as well as design variable changes. The authors developed the design synthesis method by integrating PSO with the unit truss approach to systematically design compliant mechanisms with multiple inputs/outputs. In the following section, the implementation of this method is described.

$$x_i = x_i + v_i \qquad \text{Equation 7}$$

4 IMPLEMENTATION

The design synthesis was implemented and integrated in MATLAB. The PSO algorithm follows the general structure shown in Figure 5. "DV" means design variables. $best(x)$ represents the best position p among the swarm with positions x and has $f(p) = \min(f_k)$. f_k represents the objective function values in the k^{th} iteration.

The target value f_{goal} is the desired value of the objective function, which can be a sum of weighted objective values as given in Figure 4. Usually, f_{goal} is set as zero. The maximum number of iterations for each run is given as N_{iter} to avoid a dead loop. Automatic termination of the search process is applied when the target is reached as given in Equation 8 or the convergence deviation (such as standard deviation of the search solutions) is less than the tolerance of design variables ε_{var} as given in Equation 9. ε_{obj} is the tolerance of objective function, and ε_{var} is the tolerance of design variables.

$$\left| f_g - f_{goal} \right| \le \varepsilon_{obj} \qquad \text{Equation 8}$$

$$mean(\|v\|) \le \varepsilon_{\text{var}} \qquad \text{Equation 9}$$

The velocity inertia w_k linearly varies from w_{start} to w_{end}. The start velocity inertia w_{start} and the end velocity inertia w_{end} are given based on experience. The recommended values are given as $w_{start} = 0.9$ to $w_{end} = 0.4$. Increasing w_{start} and w_{end} will make the particles jump with bigger steps and have less probability to converge. The cognition learning factor φ_1 and the social learning factor φ_2 balance the processes for global search and local search. The recommended choices of φ_1 and φ_2 are integer 2.

The minimum manufacturable strut size $x_{\min}$ is the lower bound of design variables. The maximum strut size $x_{\max}$ is the upper bound of design variables. Typically, this parameter is based on the constraints imposed by the selected manufacturing process. For the SLA 3500 machine, for example, $x_{\min}$ is set as $0.7mm$ based on experiments and $x_{\max}$ is given as $8.0mm$ in order to consider the struts as beams.

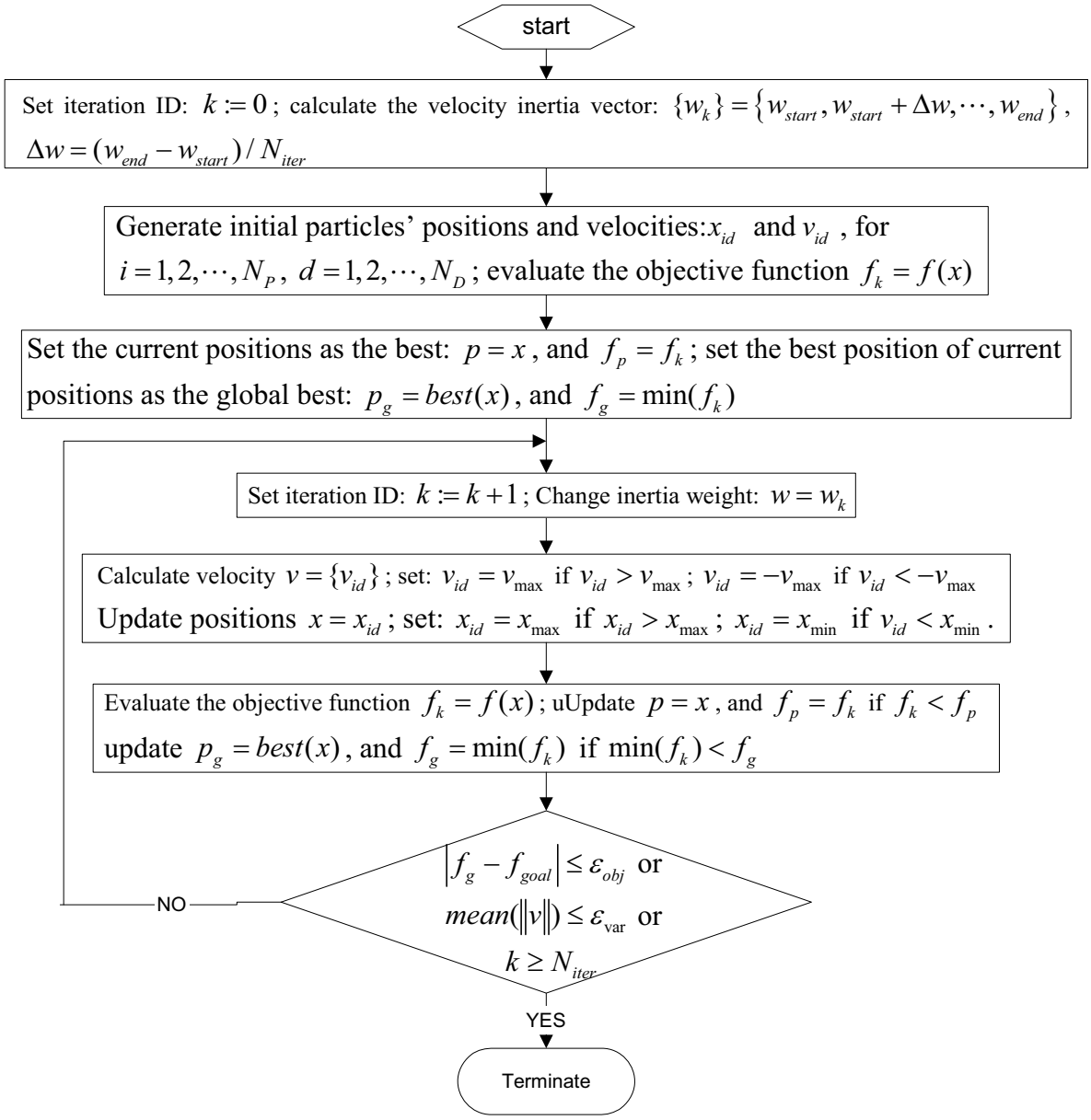

f_{goal}	- Target value to achieve	N_{iter}	- Number of iterations	w_{start}	- Start velocity inertia
w_{end}	- End velocity inertia	φ_1	- Cognition learning factor	φ_2	- Social learning factor
ε_{obj}	- Tolerance of objective function	ε_{var}	- Tolerance of DV	$x_{\min}$	- Lower bound of DV
$x_{\max}$	- Upper bound of DV	N_D	- Number of DV	N_P	- Number of particles
$v_{\max}$	- Maximum moving velocity	N_{iter}	- Number of iterations		

Figure 5. Implementation of PSO for adaptive cellular structure design

N_D is the number of design variables, in another words, the number of struts. The number of particles, N_P, is given based on experience. Usually it is given as 20. A larger number of particles N_P can make the search result more reliable, but this also requires more iterations to converge.

The maximum moving velocity $v_{\max}$ is usually set as the difference between the upper bound and lower bound of design variables. In fact, $v_{\max}$ can be looked as the largest allowable jump step for particles.

5 VALIDATION

In order to validate the integration of the unit truss approach and particle swarm, we choose to compare the results of its implementation on a simple problem with those from the Optimality Criteria (OC) with homogenization method [21]. The validation example is shown as in Figure 6, which is a 300x150x5 mm cantilever plate with elastic modulus of $200MPa$. It is loaded with a 1 N force at a distance 40 mm from the top edge. The goal is to optimize the material distribution with a material usage of 30% of the domain volume for minimum deflection.

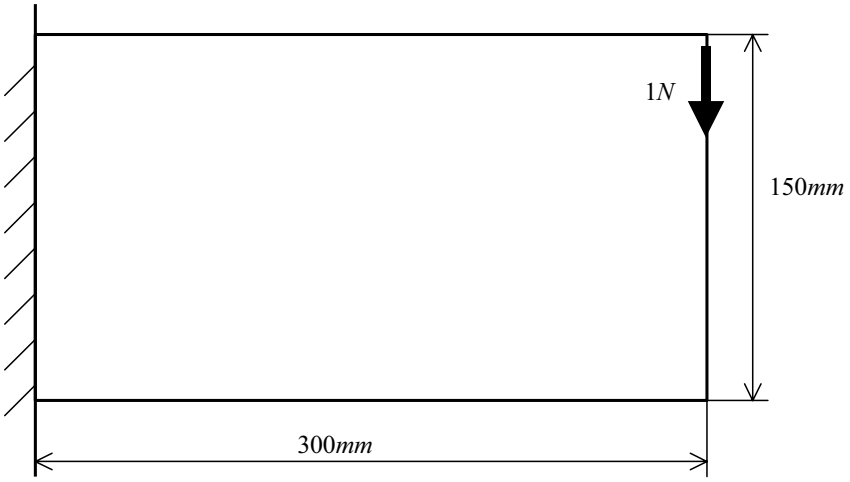

Figure 6. Validation example for design synthesis

The solution generated by the Optimality Criteria and homogenization method for a desired average density of $\rho = 0.3$ is shown in Figure 7. In the homogenization problem, each element has one design variable, the density. Elements are 10x10 mm in size, thus the plate has 450 elements and variables. The 99-line code of OC with homogenization method by Sigmund [37] is used to solve the problem for the comparison. Convergence is achieved within 80 iterations - about 4 minutes elapsed time on a standard PC with a 2.4GHz processor. The maximum deflection found using this solution strategy was 1.9 mm.

The solution of the same problem using our PSO method with unit truss approach for the average density $\rho = 0.289$ [*] is presented in Figure 8. This structure has the same thickness (5mm) as that for homogenization method. The unit truss problem has 58 struts, wherein the strut width is the sole variable for each. The PSO with unit truss approach is run for 200 iterations with 20 particles and the resulting deflections ranged between 1.3 mm and 1.8 mm. In each iteration, the objective function is evaluated 20 times since 20 particles are used. For 200 iterations and 20 particles, the objective function is evaluated 4000 times, and about 12 minutes elapsed time was required to solve the problem. The thin lines shown in Figure 8 represent the struts with negligible width.

[*] The constraint $\rho \leq 0.3$ is applied in the search process by using penalty function and considered as a continuous function; hence, the search result may not have exactly $\rho = 0.3$.

Figure 7. Result from homogenization method

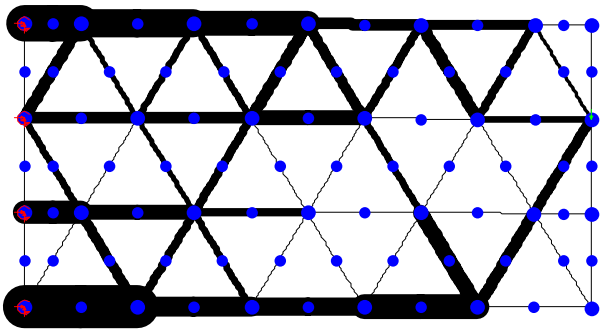

Figure 8. Result from the new design synthesis approach

The unit truss approach returned a solution that had a slightly smaller area and deflection than that of the homogenization method. Though the unit truss problem had an order of magnitude fewer variables, it took 3 times longer to reach a solution. The PSO with unit truss approach took many more runs (4000 runs; 200 iterations with 20 particles) to evaluate the objective functions than the OC with homogenization method (80 runs). The main reason for this is that the OC uses gradient and Hessian matrices as the heuristic information during the search process, while the PSO does not use either of them. Regarding the geometry of the solutions, the result with the unit cell approach is manufacturable, while the gray elements in the result from homogenization are not manufacturable. This is a limitation of the homogenization method.

Both the homogenization method and the unit truss approach have their advantages and disadvantages; however, the homogenization method with optimality criteria is very effective for continuous convex design domain. It needs gradients and Hessian matrices, which are obtained only with expansive efforts and computational resources. The homogenization method also presents results that are not manufacturable. For the validation example above, the design domain is continuous with design variables varying from 0.01 to 1.0, but those elements with design variables ranging between 0.01 and 1.0 are not manufacturable or do not physically exist. To precisely represent the physical meaning, the design variables are not continuous and the design domain is discrete. Moreover, the gradients and Hessian matrices used for homogenization method are obtained by an approximation with power-law interpolation [21]. This power-law interpolation cannot precisely represent the true physical behavior of microstructures. When solving 3-D structural problems, the number of design variables for homogenization method is scaled much more dramatically than unit truss approach. For example, 8000 microstructures (lateral size 10mm) are needed to represent a 3-D domain with lateral size 200mm. As a result, 8000 design variables are required. The research about 3-D structural homogenization method has not been explored as extensively as 2-D homogenization method because of those difficulties.

The unit truss approach with particle swarm optimization can solve problems with discrete design domains. It does not require the gradients and Hessian matrices, which makes it a convenient method for users. Furthermore, the number of design variables in the unit truss approach is much fewer than the homogenization method. The number of design variables is only about 11% of that of homogenization method for the validation problem. The search time of the design synthesis process should be cut significantly with the use of unit truss approach.

6 EXAMPLE PROBLEM: MORPHING WING

For further validation of our methodology, we investigated the design synthesis of a compliant mechanism that enables an entire closed-loop airfoil profile to change shape from NACA 23015 to FX60-126. The nonlinear behavior of largely compliant mechanisms under large deformation is considered. The resulting design is validated by testing its robustness and considering nonlinearity.

A morphing wing concept for AAI's Shadow shown in Figure 9 is proposed as an example problem in this research. AAI's Shadow is a small Unmanned Aerial Vehicle (UAV) for information collection [22]. The flight range and endurance of UAV are limited by the fuel storage capacity. It is greatly desired to increase the flight range and endurance without the addition of fuel. As the fuel is burned throughout the mission, the total weight of the UAV decreases. As the aircraft's weight decreases, the wings' working condition changes, and a different airfoil shape would better serve the aircraft. The airfoil geometry is desired to morph and accommodate the changing working condition for high airfoil performance. Wings with adaptive shapes can minimize the mission drag and improve the fuel efficiency. In the AAI's Shadow example studied by Gano and Renaud [23], the wing cross-section morphs from NACA 23015 to FX60-126 are as shown in Figure 11 [24]. NACA 23015, represented by the large profile, is bulky and has more capacity to store fuel as the starting cross-section. FX60-126, represented by the solid block, is slender as desired for the shape at the end of mission. The profile coordinates of NACA 23015 and FX60-126 airfoil cross-sections were obtained from UIUC airfoil data site [25].

Figure 9. AAI's shadow 400 UAV system [26]

Find: $x = \{x_1, x_2, \cdots, x_n\}$ Widths of lattice struts

Satisfy:

Bounds: interior struts – $x_i \in \left[x_{0^+}, x_{\max}\right]$

boundary struts – $x_j \in \left[x_{b\min}, x_{\max}\right]$

where, $x_{0^+} = 2.5e-4, x_{b\min} = 5.0, x_{\max} = 8.00$

$i = 2 \sim 59,88,89,91 \sim 94,99 \sim 104,106,113,114,116$

$j = 1,60\sim87,90,95,97,98,105,107\sim112,115,117$

Minimize: $f(x) = \underbrace{w_d \times (\text{mean}(SD_k))_{norm}}_{\text{mean squared deviation}} + \underbrace{w_v \times V_{norm}}_{\text{volume reduction}}$

where, $w_d = 60.0$, $w_v = 5.0$, $k = 8,12,16,24,29,33,63,69$

Figure 10. Problem formulation of compliant mechanism for morphing wing

The problem formulation of the design synthesis for the morphing wing is shown in Figure 10 [24]. The design variables are the widths x_i ($i = 1,2,...,117$) of the struts in the initial topology that has a total of 117 struts and72 nodes. Both the most left and right nodes are fixed; five pairs of equal and opposite forces are applied on the upper and lower boundary as shown in Figure 12. The design objective is to minimize the weighted sum objective value $f(x)$ of the weighted mean squared deviation $(\text{mean}(SD_k))_{norm}$ and normalized volume V_{norm}. The displacements are sampled from 8 points N_k ($k = 8,12,16,24,29,33,63,69$) on the airfoil shown in Figure 11. The desired deflections are shown as follows:

$$\delta_{8_{\text{target}}} = 6.58, \delta_{12_{\text{target}}} = 11.4, \delta_{16_{\text{target}}} = 13.7, \delta_{24_{\text{target}}} = 1.56$$
$$\delta_{28_{\text{target}}} = 2.14, \delta_{33_{\text{target}}} = 0.0, \delta_{63_{\text{target}}} = 9.43, \delta_{69_{\text{target}}} = -3.65$$

Equation 8

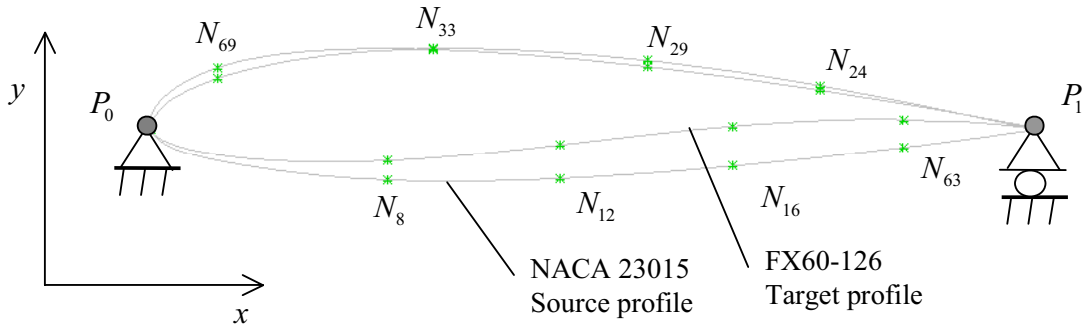

Figure 11. Airfoil morphing from NACA 23015 to FX60-126

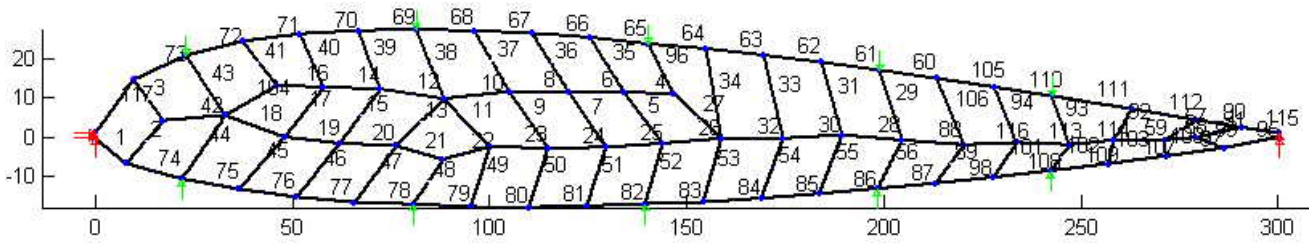

Figure 12. The initial topology for the design morphing wing

A total of 10 runs of the PSO algorithm were performed with 38,300 evaluations of the objective function for 4.81 hours of CPU time. Each evaluation of the objective function takes about 0.612 seconds. The experiment computer has an Intel P4 2.4GHz CPU and 512MB RAM. The best run produced the objective function value $f(x) = 4.37$ with the deflections at the sampled points shown in Table-1 and the resulting deformed shape is shown in Figure 13.

Table-1. Deviations between actual and target deflections at the sampled points

	Node ID	8	12	16	24	28	33	63	69
	Target	6.580	11.400	13.700	1.560	2.140	0.000	9.430	-3.650
Before synthesized	Actual	-6.397	-11.360	-13.759	-1.686	-2.250	-0.020	-9.427	3.645
	Deviation	-12.977	-22.760	-27.459	-3.246	-4.390	-0.020	-18.857	7.295
After synthesized	Actual	5.226	11.515	13.532	1.250	3.125	3.031	6.848	0.225
	Deviation	-1.354	0.115	-0.168	-0.311	0.985	3.031	-2.582	3.875

A topology cleaning process is performed on the resulting synthesized topology by removing "zero-width" struts, defined as widths close to 0.00025mm. During the cleaning process, the dangling elements are removed as well. The cleaned structure has 68 struts and 60 nodes as shown in Figure 14. After cleaning, the objective function value $f(x) = 5.012$ is a little larger than that before cleaning. This difference is caused by the removal of struts that contribute to the structure's stiffness even if their widths are very small. It is important to note, however, that this does not extensively influence our design synthesis result.

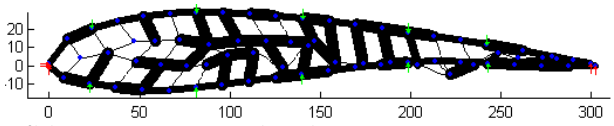

$f(x) = 4.367$, mean$(SD_k) = 2.854$, $V_{norm} = 0.302$

Figure 13. Deformed structure with five pairs of opposite forces after synthesis

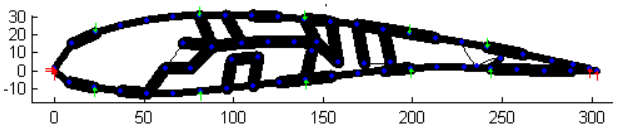

$f(x) = 5.012$, mean$(SD_k) = 3.69$, $V_{norm} = 0.264$

Figure 14. Cleaning topology by removing zero-width struts

7 CONCLUSIONS

The authors successfully developed a design synthesis method to design adaptive mesoscopic cellular structures with the use of unit truss approach and Particle Swarm Optimization algorithm (PSO). The new design synthesis method enables the analysis and design of complicated cellular structures including lightweight structure and compliant mechanisms. Axial forces, bending, torsion, nonlinearity, and buckling can be simultaneously considered. The design synthesis of adaptive cellular structures is a large-scale nonlinear problem with multiple objectives and a mixed-discrete design space. The authors formulated the design problems for both types of adaptive cellular structures, and selected PSO to systematically search for design solutions. The unit truss approach and PSO were successfully implemented and integrated in MATLAB.

The authors solved a cantilever beam problem by using both the new design synthesis method and the existing homogenization method. The resulting designs are similar in terms of average density and deflection; however, all struts in the result of the design synthesis method with the unit cell approach are manufacturable, while some of the elements in the result created with the homogenization method are not. As opposed to the homogenization method, the new design synthesis method does not need efforts to obtain gradients or Hessian matrices, and has fewer design variables. The authors demonstrated the new design synthesis method through the successful design of a compliant mechanism for morphing wing, which has multiple objectives and a nonlinear design domain.

ACKNOWLEDGEMENTS

We gratefully acknowledge the U.S. National Science Foundation, through grants IIS-0120663 and DMI-0522382, and the support of the Georgia Tech Rapid Prototyping and Manufacturing Institute member companies for sponsoring this work.

REFERENCES

[1] J. Banhart, "Manufacturing Routes for Metallic Foams," *Journal of the Minerals*, vol. 52, pp. 22-27, 2000.

[2] H. Wang, Y. Chen, and D. W. Rosen, "A Hybrid Geometric Modeling Method For Large Scale Conformal Cellular Structures," ASME Computers and Information in Engineering Conference, Long Beach, California, September 24-28, 2005, 2005, Paper Number: DETC02/CIE-34495

[3] C. C. Seepersad, "*A Robust Topological Preliminary Design Exploration Method With Materials Design Applications*," PhD, School of Mechanical Engineering, Georgia Institute of Technology, Atlanta, GA, 2004.

[4] C. B. Williams, F. Mistree, and D. W. Rosen, "Investigation of Solid Freeform Fabrication Processes for the Manufacture of Parts with Designed Mesostructure," ASME IDETC Design for Manufacturing and the Life Cycle Conference, Long Beach, California, 2005

[5] S. Kota, J. Joo, Z. Li, S. M. Rodgers, and J. Sniegowski, "Design of compliant mechanisms: applications to MEMS," *Analog Integrated Circuits and Signal Processing*, vol. 29, pp. 7-15, 2001.

[6] L. L. Howell, *Compliant mechanisms*, John Wiley & Sons, New York, NY, 2001.

[7] A. Midha, T. W. Norton, and L. L. Howell, "On the nomenclature, classification, and abstractions of compliant mechanisms," *ASME Journal of Mechanical Design*, vol. 116, pp. 270-279, 1994.
[8] D. E. Ingber, "Cellular tensegrity: defining new rules of biological design that govern the cytoskeleton," *Cell Science*, vol. 104, pp. 613-627, 1993.
[9] D. Bray, "Cell," Microsoft® Encarta® Online Encyclopedia http://au.encarta.msn.com, 2005
[10] S. A. Burns, *Recent advances in optimal structural design*: American Society of Civil Engineers, 2002.
[11] W. K. Rule, "Automatic truss design by optimized growth," *Journal of Structural Engineering*, vol. 120, pp. 3063-3070, 1994.
[12] A. G. M. Michell, "The limits of economy in frame structures," in *Philosophical Magazine Sect. 6*, vol. 8, 1904, pp. 589-597.
[13] M. P. Bendsoe, *Optimization of structural topology, shape, and material*, Springer-Verlag, Berlin Heidelberg, 1995.
[14] M. P. Bendsoe and N. Kikuchi, "Generating optimal topologies in structural design using a homogenization method," *Computer Methods in Applied Mechanics and Engieering*, vol. 71, pp. 197-224, 1988.
[15] H. Wang, "*A unit cell approach for lightweight structure and compliant mechanism*," PhD Dissertation, School of Mechanical Engineering, Georgia Institute Of Technology, Atlanta, GA, 2005.
[16] G. I. Rozvany, *Topology Optimization in Structural Mechanics*: Springer Verlag, 1997.
[17] W. McGuire, R. H. Gallagher, and R. D. Ziemian, *Matrix structural analysis*, 2nd ed, John Wiley, 2000.
[18] J. Neter, M. H. Kutner, C. J. Nachtsheim, and W. Wasserman, *Applied linear statistical models*, 4th ed, Irwin/McGraw-Hill, Chicago, Boston, Mass., 1996.
[19] P. C. Fourie and A. A. Groenwold, "The particle swarm optimization algorithm in size and shape optimization," *Structural and Multidisciplinary Optimization*, vol. 23, pp. 259 - 267, 2002.
[20] J. Kennedy and R. C. Eberhart, "Particle swarm optimization," Proceedings of IEEE International Conference on Neural Networks, Piscataway, NJ, pp. 1942-1948, 1995
[21] O. Sigmund, "A 99 line topology opitimization code written in Matlab," *Struct Multidisc Optim*, vol. 21, pp. 120-127, 2001.
[22] "Materials for lean weight vehicles: the battle for a better body," *Steel Times (UK)*, vol. 226, pp. 73-74, 1998.
[23] S. E. Gano and J. E. Renaud, "Optimized Unmanned Aerial Vehicle With Wing Morphing For Extended Range And Endurance," 9th AIAA/ISSMO Symposium and Exhibit on Multidisciplinary Analysis and Optimization, Atlanta, GA, September 4-6, 2002, 2002, AIAA-2002-5668
[24] H. Wang and D. W. Rosen, "An Automated Design Synthesis Method for Compliant Mechanisms with Application to Morphing Wings," ASME Design Mechanisms and Robotics Conference, Philadelphia, PA, September 10-13, 2006, 2006, DETC2006-99661
[25] M. Selig, "UIUC Airfoil Coordinates Database - Version 2.0," Department of Aerospace Engineering, University of Illinois at Urbana-Champaign, Urbana, Illinois 61801 http://www.ae.uiuc.edu/m-selig/ads.html, August 10, 2005, 2005
[26] "Shadow 400 UAV system," AAI Corporation http://www.aaicorp.com, September 13, 2005